Ceramics International 42 (2016) 9703–9711

Contents lists available at ScienceDirect

Ceramics International

journal homepage: www.elsevier.com/locate/ceramint

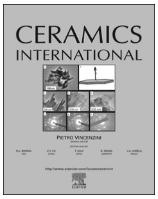

Thermo-mechanical characterization of a silica-alumina refractory concrete based on calcined algerian kaolin

F. Benali [a], M. Hamidouche [b], H. Belhouchet [a,c,*], N. Bouaouadja [a], G. Fantozzi [d]

[a] Laboratory of Non Metallic Materials, Institute of Optics and Precision Mechanics, University Ferhat Abbas Setif 1, Setif 19000, Algeria
[b] Research Unit on Emerging Materials (RUEM), University Ferhat Abbas Setif l, Setif 19000, Algeria
[c] Physics Department, Faculty of Sciences, University Mohamed Boudiaf – M'sila, M'sila 28000, Algeria
[d] Laboratory MATEIS (UMR CNRS 5510), Bat. Blaise Pascal, INSA, Villeurbanne, France

ARTICLE INFO

Article history:
Received 2 February 2016
Received in revised form
8 March 2016
Accepted 8 March 2016
Available online 9 March 2016

Keywords:
C. Creep
Calcined kaolin
Thermo-mechanical behaviour
Thermal shock
Refractory concrete

ABSTRACT

The aim of this work is to study the thermo-mechanical behaviour (bending and compressive tests, creep and thermal shock resistance) of a refractory concrete based on local kaolin grogs and aluminous cement. Strength tests revealed a behaviour that is almost linear elastic for temperatures up to 800 °C and visco-plastic at 900 °C. A crack bridging strengthening process was observed at 800 °C. The creep tests were carried out at different temperatures between 1000 and 1150 °C using stresses in the range (0.75–2.76 MPa). The stress exponent was about 1.255. Microscopic observations suggested an intergranular creep mechanism.

A water quenching test was used for estimating the thermal shock resistance of the material. The tested samples supported 80 cycles of standardized cyclic thermal shock without failure. Ultrasonic measurements were applied in order to evaluate the of ultrasonic velocity changes after these thermal shock tests. Strength degradation of the samples was evaluated using two models based on ultrasonic velocity changes during test and compared with the experimental values.

1. Introduction

Castable refractories are the simplest to implement among monolithic refractories. They generally consist of a mixture of cement and refractory aggregates. They can be classified in various ways. According to their chemical constituents, those based on alumina and alumina-silicate aggregates are distinguished from others based on basic refractory oxides aggregates [1–3]. In recent years, the use of monolithic refractories evolved considerably. They are generally used in numerous installations exposed to high temperatures (steelmaking, cement industry, petrochemical and nuclear industries) [4–6].

In all these applications, the life of a refractory concrete passes through three main phases. During the first putting in service, the concrete temperature rises and causes damages such as cracks or failures due to dehydration process (in the case when the heating rate is high), leading to microstructural changes and/or shrinkage mechanism. As a consequence, the second phase corresponds to the cyclic services conditions: cracks apparition and/or propagation can occur due to thermal shock enhanced by thermal cycles [7]. In the final phase after complete cooling, the structure is inspected to evaluate the damage induced by the material's cycles putting in service, the decision to repair or eventually change the refractory layer is based on this evaluation [4,8].

For understanding and predicting the changes in the refractory's concrete behaviour during putting in service, the material thermo-mechanical study is required. This study provides data for modelling and simulating thermo-mechanical behaviour.

In many applications, the thermal shock resistance dictates the refractory performance in many applications. In many instances, a twofold approach, i.e. (1) thermal shock damage resistance or (2) thermal stress fracture initiation [7] is used to characterize thermal shock behaviour of refractories.

The refractory thermal shock resistance can be characterised by quenching appropriate specimens from a furnace at elevated temperature into a medium such as water, oil, or fused salts maintained at a lower temperature. The most commonly used test is water quenching. Thermal quenching can lead to the crack nucleation and/or crack propagation resulting in loss of strength. Cracks formation has a profound influence on the ultrasonic velocity and the material Young's modulus. By measuring these properties, we can monitor the development of the thermal shock damage level.

---

* Corresponding author at: Physics Department, Faculty of Sciences, University Mohamed Boudiaf – M'sila, M'sila 28000, Algeria.
E-mail address: hbelhou@yahoo.com (H. Belhouchet).

http://dx.doi.org/10.1016/j.ceramint.2016.03.059
0272-8842/© 2016 Elsevier Ltd and Techna Group S.r.l. All rights reserved.

Many authors focused on determining mechanical properties of heated refractory concrete at room temperature. Compressive, tensile and bending tests were used to determine mechanical characteristics of the material [9–12]. Other studies were oriented toward understanding the thermo-mechanical behaviour [13–17]. Besides, a modelling of this behaviour was made using experimental data as we intend to do in our work for the thermal shock testing [18]. The silica-alumina refractories thermo-mechanical behaviour was examined in some of these works [18]. The behaviour of such material is strongly influenced by the vitreous phase. At particular temperature ranges, a positive effect on the mechanical strength and fracture toughness can take place by strengthening mechanisms at the cracks tips [19]. At higher temperatures, the softening of the vitreous phase generates a visco-plastic phenomenon, clearly visible on stress–strain curves [20].

The effect of the amorphous phase is very important on the material creep behaviour, especially when its quantity is important and uniformly distributed [11]. Its effect on the vitreous phase on the thermal shock resistance can be beneficial from two different points of view. On one hand, it enables to release the residual thermal stresses, and on the other, it has a strengthening effect by inducing a cracks bridging process. It therefore improves the refractory behaviour towards brutal temperature variations [16].

During service, the refractories are exposed to extremely severe thermo-mechanical conditions caused by high temperatures combined with constant or repeated mechanical solicitations [17]. Therefore, they must be tested for their liability in similar conditions before being used in practical situations.

In this work we will investigate the thermal and the thermo-mechanical properties of a silica-alumina refractory concrete prepared from calcined Algerian kaolin with addition of andalusite waste fillers and fused cement. High temperature mechanical tests; creep and thermal fatigue tests were undertaken. The modulus of rupture at high temperature, creep behaviour and thermal shock fatigue are characterized and discussed.

2. Experimental procedure

2.1. Used materials

The mixture used to make our refractory is selected among various batches of fused cement called “Ciment Fondu” from Kernos (France), andalusite waste fillers and calcined kaolin (DD3, Djebel Debbagh, Algeria) (chamotte) [19]. The chemical composition determined by X-ray fluorescence (XRF) of prepared concrete and the refractory compositions are summarized in Tables 1 and 2 respectively.

Table 1
Formulation of the prepared concrete (in wt%).

Components	The prepared concrete
SiO_2	36.37
Al_2O_3	52.37
CaO	4.10
Fe_2O_3	2.11
MgO	0.32
MnO	0.26
K_2O	0.31
ZrO_2	0.01
Na_2O	0.20
TiO_2	0.72
Cr_2O_3	0.01
SO_3	0.61
L. O. I.	2.63

Table 2
Compositions (in wt%) of the silico-alumina refractory concrete based on calcined Algerian kaolin.

Components	**wt(%)**
Fused cement ($\phi \leq 40$ µm)	7
Andalusite ($\phi \leq 0.2$ mm)	38
Calcined Kaolin ($0.135 < \phi < 1.25$ mm)	10
Calcined Kaolin ($1.6 < \phi < 3.5$ mm)	45

The andalusite particle size distribution of the andalusite powder was investigated using a laser granulometer (Malvern Mastersizer 2000) and ethanol as a solvent (Riedel-de Haën 96%). The obtained distribution is presented in Fig. 1. It appears that the used andalusite has a monomodal and a homogeneous distribution with an average particle size (d_{50}) of 7.3 µm. It mainly composed of large and small grains with sizes ranging from 0.557 to 60 µm. Fig. 2 confirms the results of particle size distribution; we see that there is a good dispersion of particles and the grains are formed by irregular shape with different size. A specific area determined by BET (Brunauer–Emmitt–Teller) represent a high relatively value of 6.9 m^2/g.

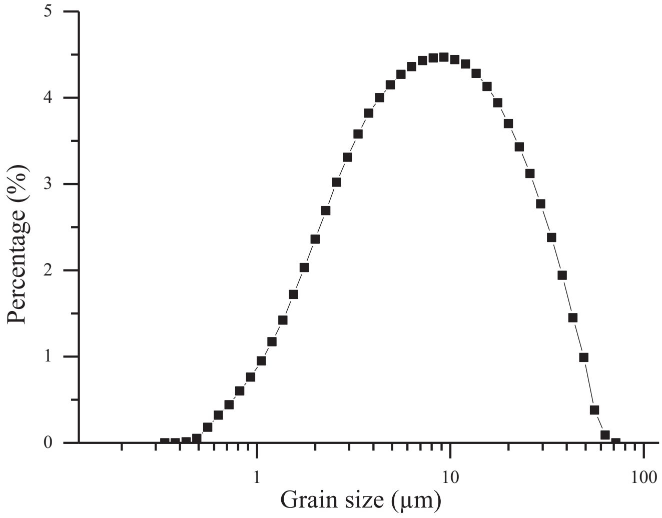

Fig. 1. Particle size distribution of crushed andalusite powder.

The refractory castable samples were prepared according to the compositions represented in Table 2. A 91 wt% well–graded aggregates were mixed with the fused cement and adequate amounts of distilled water according to the standard “good ball in hand” ASTM C-860 method [22]. The mixed batches were then cast into 150 × 30 × 30 mm^3 bars for creep studies as well as into 30 mm diameter cylindrical samples with 50 mm height for thermal shock tests according to DIN 51 068 [23]. The Samples were left in their moulds at 98% relative humidity for 24 h. They were then demoulded, and further immersed during 3 days under water, followed by drying at 110 °C for 24 h. Finally, the samples were subjected to firing at 1450 °C in an electric furnace for 2 h.

The obtained samples were tested by cold crushing and bending using a Zwick/Roelle 50 machine. They were subjected to a Grindo–Sonic test for the determination of the dynamic Young modulus. The absolute and bulk densities were determined using a helium pycnometer apparatus (MICROMETRICS ACCUPYC 1330) and a porosimeter apparatus (MICROMERITICS 9300) respectively. We also used a selective dissolution in fluoridric acid in order to quantify the amount of the glassy phase contained in the recycled andalusite and the kaolin chamotte. The results of the above cited tests are summarized in Table 3.